Surgical and Radiologic Anatomy (2022) 44:759–766
https://doi.org/10.1007/s00276-022-02948-1

ORIGINAL ARTICLE

Subarachnoid space of the optic nerve sheath and intracranial hypertension: a macroscopic, light and electron microscopic study

A. Durouchoux[1] · D. Liguoro[2,4] · M. Sesay[3] · L. Le Petit[2] · V. Jecko[2]

Received: 12 October 2021 / Accepted: 14 April 2022 / Published online: 4 May 2022

Abstract

Purpose The optic nerve (ON) is an extension of the central nervous system via the optic canal to the orbital cavity. It is accompanied by meninges whose arachnoid layer is in continuity with that of the chiasmatic cistern. This arachnoid layer is extended along the ON, delimiting a subarachnoid space (SAS) around the ON. Not all forms of chronic intracranial hypertension (ICH) present papilledema. The latter is sometimes asymmetric, unilateral, or absent. The radiological signs of optic nerve sheath (ONS) dilation, in magnetic resonance imaging, are inconsistent or difficult to interpret. The objective of this study was to analyze the anatomy, the constitution, and the variability of the SAS around the ON in its intraorbital segment to improve the understanding of the pathophysiologic mechanism of asymmetric or unilateral or absent papilledema in certain ICH.

Methods The study was carried out on nine cadaveric specimens. In four embalmed specimens, macroscopic analysis of the SAS of the ONS were performed, with description about density of the arachnoid trabecular meshwork in three distinct areas (bulbar segment, mid-orbital segment and the precanal segment). In three other embalmed specimens, after staining of SAS by methylene blue (MB), we performed macroscopic analysis of MB progression in the SAS of the ONS. Then, in two non-embalmed specimens, light and electron microscopy (EM) analysis were also done.

Results On the macroscopic level, after staining of SAS, we found in all cases that MB progressed on 16 mm average throughout the SAS of the ONS without reaching the papilla. In four embalmed specimens, in the SAS of the ONS, the density of the arachnoid trabecular meshwork showed inter-individual variability (100%) and intra-individual variability with bilateral variability (50%) and/or variability within the same ONS (88%). On the microscopic level, the arachnoid trabeculae of the ONS are composed of dense connective tissue. The EM perfectly depicted its composition which is mainly of collagen fibers of parallel orientation.

Conclusion The variability of the SAS around the ONS probably impacts the symmetrical or asymmetrical nature of papilledema in ICH.

Keywords Optic nerve sheath · Subarachnoid space · Papilledema · Intracranial hypertension · Anatomy

Introduction

The optic nerve (ON), cranial nerve II, is not actually a cranial nerve but an extension of the central nervous system via the optic canal to the orbital cavity. The optic nerve sheath (ONS) is the longest of the transbasal sheaths and has three segments: intracranial, intracanalicular and intraorbital. The meninges form the ONS, whose arachnoid layer is in continuity with that of the chiasmatic cistern [3, 20]. The arachnoid layer is extended along the ON, thus delimiting a subarachnoid space (SAS) around the ON. This SAS contains a complex system of arachnoid trabeculae and septa [11].

✉ A. Durouchoux
arthur.durouchoux@icloud.com

1 Neurosurgery B Department, University Hospital Bordeaux, Bordeaux, France

2 Neurosurgery A Department, Bordeaux Hospital, Bordeaux, France

3 Neuroanesthesia, Bordeaux Hospital, Bordeaux, France

4 Department of Anatomy, University of Bordeaux, Bordeaux, France

Not all forms of chronic intracranial hypertension (ICH) present papilledema. In idiopathic intracranial hypertension (IIH), there is an average of 4% of patients with unilateral or asymmetric or absent papilledema [1, 2]. This phenomenon is rare and of unknown pathophysiology. The radiological signs of ONS dilatation, in magnetic resonance imaging, are sometimes inconsistent or difficult to interpret [5, 18, 22].

The objective of this work was to study the anatomy, the constitution, and the variability of the SAS around the ON in its intraorbital segment to improve the understanding of the pathophysiologic mechanism of asymmetric or unilateral or absent papilledema in certain ICH.

Materials and method

Our anatomical study was carried out on nine cadaveric specimens (Anatomy Department of Bordeaux, Medical University of Bordeaux).

Two specimens were embalmed in 10% formalin solution before dissection. Four ON were removed, then sectioned longitudinally using a surgical microscope (ZEISS OPMI 6-CFC Microscope, F170, 10×/22B binoculars). These samples were used for macroscopic analysis (Nikon camera D3200 18–55 mm/f 3.5–5.6) and an electron microscopy analysis (Bordeaux Imaging Center—Electronic Imaging, University of Bordeaux).

Two subjects were prepared with staining of the arteries and veins, in red and blue respectively, with a mixture of latex and dye (Cis-1.4 Polyisoprene Pebeo centrifuged natural latex; Colorex Pebeo acrylic ink). They were then embalmed in a 10% formalin solution before dissection. Four ON were removed, then sectioned longitudinally using a surgical microscope (ZEISS OPMI 6-CFC Microscope, F170, 10x / 22B binoculars). These samples were used for a macroscopic analysis only (Nikon camera D3200 18–55 mm/f 3.5–5.6).

From two non-embalmed specimens, it was possible to remove four ON which we preserved in a solution of glutaraldehyde (2.5% glutaraldehyde mixed with 0.1 M cacodylate buffer, pH at 7.2). Each ON was cut in its retrobulbar orbital part about 4 mm from the eyeball, then analyzed in semi-fine millimeter section under a light microscope (LM) to select areas of interest for analysis by EM. The samples intended for EM were cut with a vibratome (Leica VTS1200S) with a thickness of 500 µm, the sections were then treated by washing then staining with 1% osmium tetroxide (OsO4) then included in epoxy resin before being cut with an ultramicrotome in ultra-fine sections of 70 nm.

The areas of interest selected in LM were then analyzed by EM by the "Bordeaux Imaging Center—Electronic Imaging" laboratory of the University of Bordeaux (Electron microscope, Hitachi H7650, Tokyo, Japan; equipped with an Orius 11Mpx camera Gatan, Paris, France).

Three other subjects were prepared with a subarachnoid injection, at the cervical spinal level, by physiological saline stained with methylene blue (MB). Then, the parietal bone was opened via trephine to embalm the brain in a 10% formalin solution. After 1 week, we performed the dissections for a macroscopic analysis of the progression of the MB within the SAS.

The dissections were carried out according to the same protocol. We started with a circular and bilateral skin incision from the nasion to the inion. This was followed by a circular craniotomy along the incision path, via the frontal tuberosities, the lower part of the parietal bone and the external occipital protuberance. The incision of the dura was circular and bilateral, crossing the superior sagittal sinus and the falx cerebri. Part of the brain parenchyma was then resected to visualize the anterior and mid skull base, including the roof of the orbit, the anterior clinoid process, the ON, and the optic chiasm. The dura was detached and incised until the entrance of the optic canal. We realized an osteotomy of the roof, lateral wall, and medial wall of the orbit to expose the periorbita, an anterior clinoidectomy and an osteotomy of the optic canal. Then, the periorbita was opened, for ablation of the retro bulbar intraorbital fat and oculomotor muscles. We performed a monobloc resection of the eyeball with the ON and its sheath. A transverse and posterior section of the eyeball was done while preserving the posterior pole of the sclera with the optic papilla.

We performed different analyses:

- A macroscopic analysis of the progression of MB in the SAS of the ONS, by measuring the distance between the optic disc and the limit of progression of MB.
- A macroscopic study of the density of the arachnoid trabecular network of the SAS into the ONS, by description of three stages of density (low, medium, high), by a single observer, in three distinct parts of the ONS (bulbar segment, mid-orbital segment and the precanal segment).
- Light and electron microscopic study of the architecture of the SAS.

Results

Macroscopic study

Samples taken from 9 cadaveric specimens allowed the analysis of 18 ON. Macroscopically, we were able to identify in all specimens the arachnoid within the ONS with a SAS containing CSF. The dura was continuous with the intraorbital content. The inner layer of the dura extends into the

ONS and the outer layer of the dura extends into a fibrous membrane stuck to the bone, the periorbita.

After staining the vessels, we found in all ON the ophthalmic artery which penetrated underneath the ON before becoming the central artery of the retina which ran from the ON at its center to the optic papilla. There was also a rich pial vascularization around the ON (Fig. 1).

The longitudinal section depicted, in all ON, a perioptic SAS which was rich in arachnoid trabeculae and septa. The arachnoid trabeculae were very well visualized, they formed a wire mesh network with meshes of variable size. This wire mesh network, very dense in places, looked like partitions. The widest segment of the ONS was located at the retrobulbar level, in this zone the arachnoid network, trabecular, seemed to densify near the optic papilla (Fig. 1).

In four specimens (four with formalin, two without staining and two with staining of the vessels), the density of the arachnoid trabecular meshwork showed inter-individual variability (100%) and intra-individual variability with bilateral variability (50%) and/or variability within the same ON (88%). Density of the arachnoid trabecular meshwork was also studied on 3 distinct areas of the ONS to detail the variability within the ONS (Table 1). Among these 8 ON, 5 had a higher density of arachnoid trabeculae at the retro-ocular level (62.5%), 1 had a constant density throughout the ONS (12.5%) and 2 had a lower density at the mid-ocular level (25%).

Staining of the SAS with MB allowed the analysis of CSF progression from the intracranial SAS to the ONS (Fig. 2). We noticed, in two specimens, that the progression of the MB was from the intracranial SAS towards the ONS crossing the optic canal. CSF progressed partially in the SAS in all ONS. Thus, the MB progressed, in all cases, only about 1–2 cm in front of the optic canal without reaching the optic papilla.

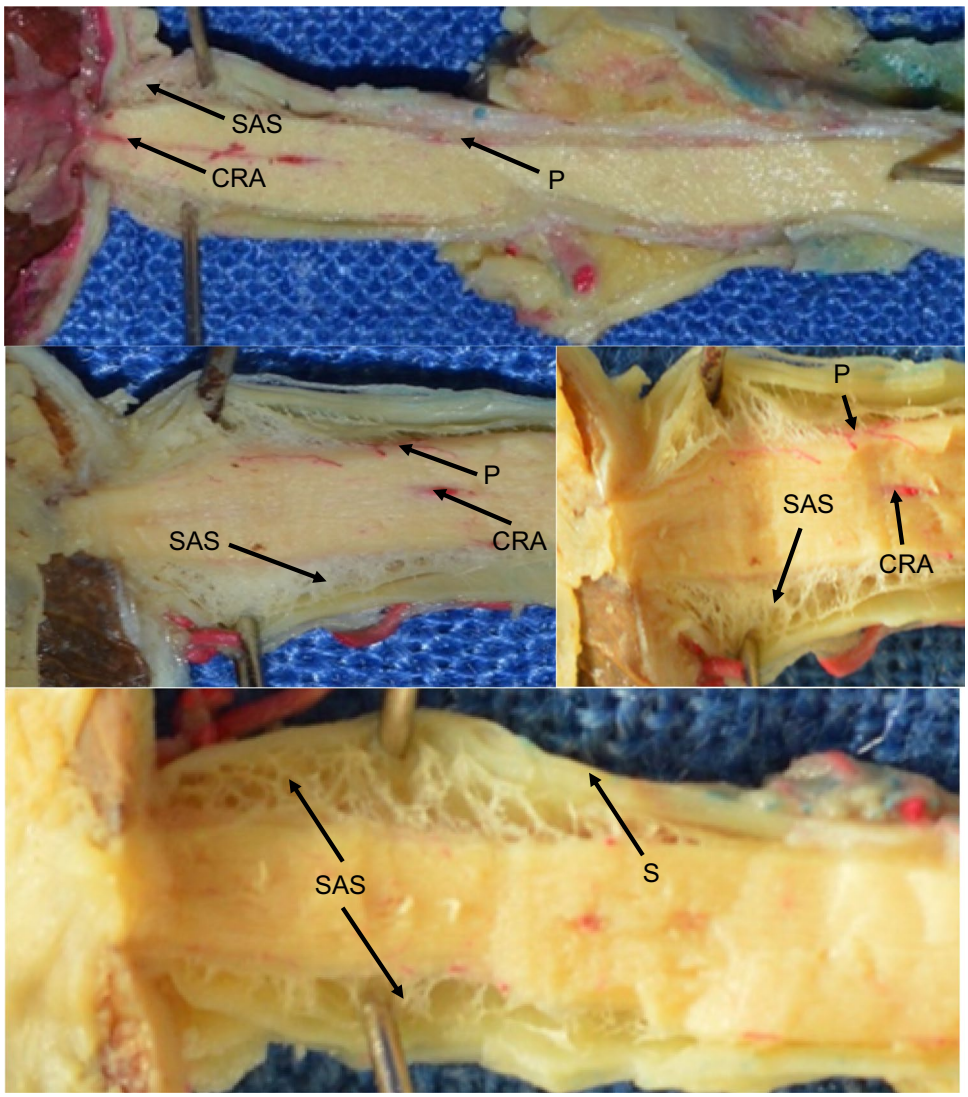

Fig. 1 Longitudinal sections of dissected optic nerves. Vascularization, sheath and subarachnoid space. *P* pia mater, *CRA* central retinal artery, *SAS* subarachnoid space, *S* optic nerve sheath

Table 1 SAS variability in 8 ONS, on three distinct parts of the intra-orbital segment

Segment (*n*)	Low density, *n* (%)	Medium density, *n* (%)	High density, *n* (%)
Bulbar segment (8)	0 (0%)	3 (37.5%)	5 (62.5%)
Mid-orbital segment (8)	4 (50%)	4 (50%)	0 (0%)
Pre-canalicular segment (8)	4 (50%)	2 (25%)	2 (25%)

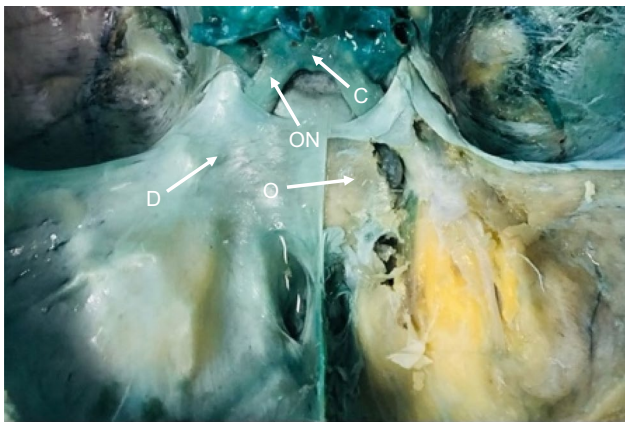

Fig. 2 Intracranial subarachnoid spaces colored in blue. *ON* optic nerve II, *C* optic chiasm, *D* dura, *O* orbit

The 6 ON removed after staining the SAS were used to analyze the distance between the optic papilla and the progression of staining within the ONS. This distance was on average 16 mm (minimum 14 mm, maximum 18 mm) (Fig. 3).

Light and electron microscopic study

LM and EM analysis were performed on eight ON (four with formalin, four without formalin). Millimeter "semi-thin" sections were analyzed by LM (Fig. 4) to select areas of interest for analysis by EM.

The EM made it possible to analyze the SAS of the ONS and describe its spatial micro-organization. This consisted of arachnoid trabeculae and some septa. Figure 5 shows the trabeculae in longitudinal or cross section depending on the direction of the cut.

Fig. 3 Subarachnoid space of the optic nerve sheath colored in blue. *ON* optic nerve II, *B* blue dye, *D* optic disc, *S* optic nerve sheath

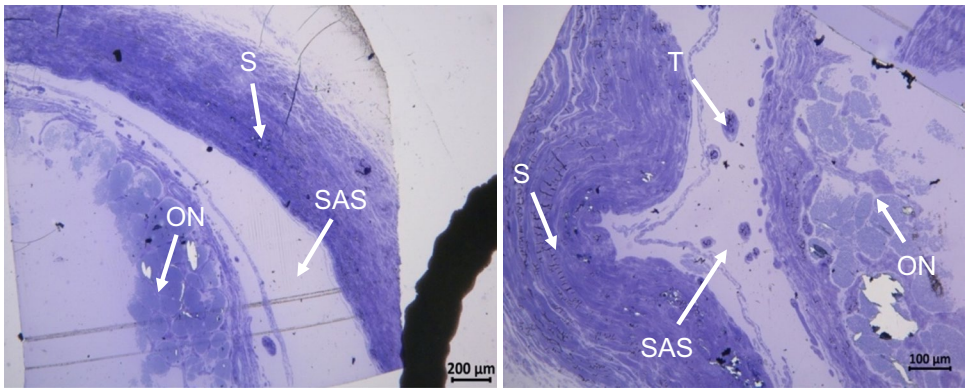

Fig. 4 Subarachnoid space of the optic nerve sheath, semi-thin sections (OM). *ON* optic nerve II, *S* optic nerve sheath, *SAS* subarachnoid space, *T* arachnoid trabecula

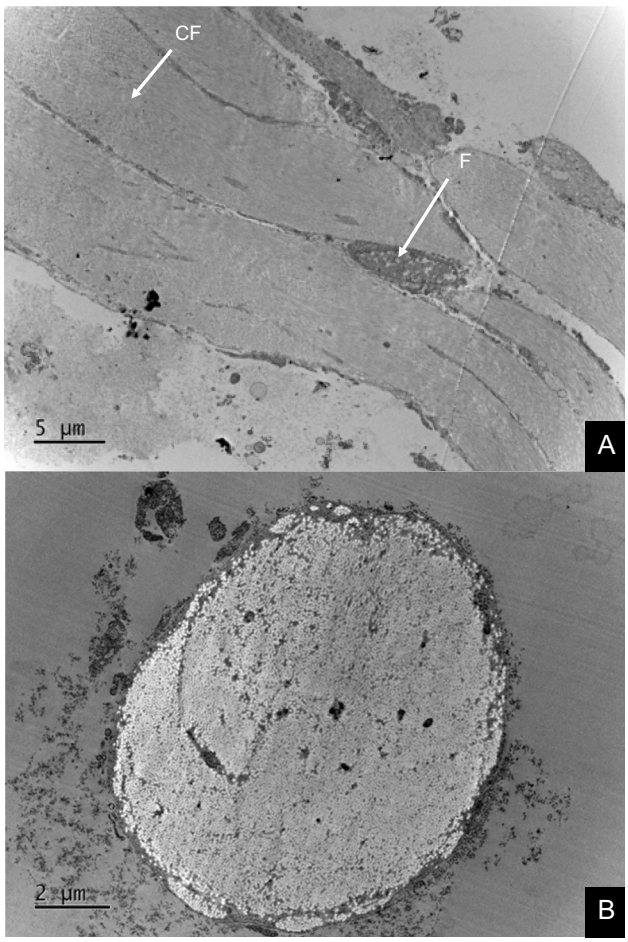

Fig. 5 Arachnoid trabeculae in longitudinal and cross sections. *A* arachnoid trabecula in longitudinal section, *CF* collagen fibers, of parallel organization, *F* fibrocyte, *B* arachnoid trabecula in cross section

The arachnoid trabeculae consisted mainly of collagen fibers, organized in very dense fiber, separated by rare fibrocytes. The trabeculae were of varying diameters, ranging from 5 to 70 µm. Under EM, the collagen fibers were recognizable by the longitudinal alignment of tropocollagen

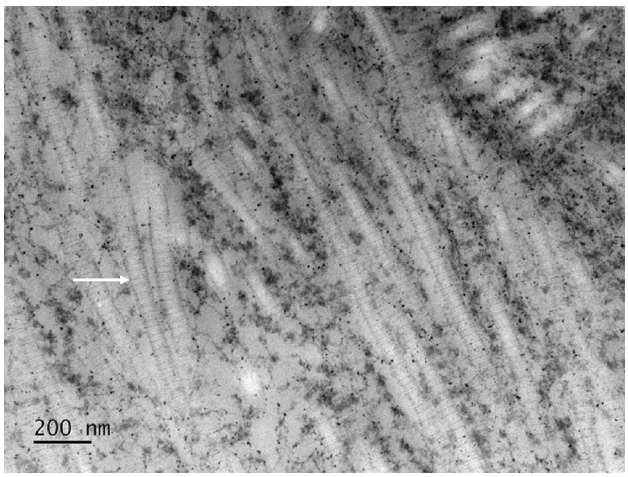

Fig. 6 Collagen fibers in EM. Arrow: characteristic periodicity of 65–70 nm of the tropocollagen chains constituting the fibrillar collagen, "D period" giving an appearance of striation in transmission electron microscopy

chains with a characteristic periodicity of around 70 nm (Fig. 6).

The ON arachnoid consisted of dense connective tissue organized in either parallel or reticular fiber of collagen. The collagen fibers were arranged in very thick fiber of parallel orientations within the arachnoid trabeculae and were mostly reticular or even disorganized within the outer layer of the arachnoid.

Discussion

ICH is manifested by headache, visual eclipse, tinnitus, diplopia, loss of visual acuity, and papilledema. Progression to reversible blindness is possible [4]. In IIH, there is an average of 4% of patients with unilateral or asymmetric papilledema [1, 2]. This phenomenon is rare and of unknown pathophysiology.

Our analysis of stained SAS showed a partial CSF progression in the SAS of the ONS. Macroscopic and microscopic analysis showed a composition rich in arachnoid trabeculae and in septa. EM analysis confirmed the dense collagen composition of the arachnoid trabeculae, organized in thick fibers, suggesting stress by mechanical tensions.

Our pathophysiologic hypothesis is the existence of some micro-partitions in the SAS of the ONS in his intraorbital segment. This SAS appears to be subdivided and sometimes appears partitioned by the reticular network of trabeculae and septum-shaped structures. These partitions could slow down the CSF flow [16] or even trap the CSF in the SAS [19] and may alter the ophthalmological clinical presentation of certain ICH.

In EM analysis, we observed the presence of dense connective tissues rich in collagen fibers in the ONS. The arachnoid trabeculae of the SAS of the ONS were composed of parallel collagen fibrils grouped together in very thick fibers. The composition of which seemed comparable to that of the connective tissues of other systems, especially the musculoskeletal system in comparison to ligaments and tendons. The parallel organization of collagen fibers, in thick fibers, seemed specifically adapted to the transmission of mechanical forces and/or constraints [15, 17]. Physiologically, there are a CSF flow in the SAS of the ONS and the SAS is subject to physiological variations in intracranial pressure. The ONS being distanced and dilated according to the subarachnoid pressure [16]. This could explain the micro-architecture of the trabeculae.

In the literature, similar LM and/or EM analysis were carried out in rabbit, sheep, monkey, and human (Table 2) [6–14, 16, 19, 21]. Staining of the SAS in blue has previously been performed in monkeys by Hayreh et al. in 1965 [7]. To our knowledge, our study provided the first analysis with staining of the SAS of the ONS in human.

Our results in LM and EM agree with those of Killer et al. in 2003 [12]. Their analysis revealed a complex system of trabeculae and arachnoid septa that divided the SAS of the ONS which may have a role in CSF hydrodynamics. In 2006, in another study, they suggest the presence of local trapping of the CSF [13]. Tsutsumi et al. in 2021 described, by a MRI and anatomical study, a hyperintense areas in the intraorbital ON detected on T2-weighted sequences corresponding to perivascular spaces of the ON and central retinal artery. These may be collapsed and difficult to identify macroscopically on cadaver specimens [21].

Unilateral or asymmetric papilledema has also been analyzed during an anatomical study in monkeys by Hayreh et al. in 1968 [6]. The mechanisms evoked were then a unilateral compression of the ON or an asymmetric adhesion of the chiasmatic cistern. These results agreed a few years later with those of Liu et al. in 1993 [16], during an anatomical study in humans reproducing an ICH. Their iterative measurements of intracranial and subarachnoid pressures around the ON, revealed an asymmetry in the peri optic pressure measurements.

In a study of the IIH with unilateral or asymmetric papilledema, Huna-Baron et al. in 2001 [8] found no macroscopic difference in the ON on CT or MRI. However, the hypothesis of a microscopic difference in the SAS of the ONS could also be evoked. This hypothesis was also proposed by Killer et al. in 2007 [14] based on a scan and cisternographic study in three patients presenting an IIH with asymmetric papilledema. This same author described in 2003 [12], in a human anatomical study, an EM analysis of the architecture of the SAS around the ON.

Table 2 Revue of the literature about ON, its sheath, ICH and papilledema

Year	Author	Subjects (n)	Macroscopy, microscopy (LM/EM)	Other methods
1965	Hayreh [7]	Monkeys	Macroscopy	Staining by MB of the ONS
1967	Jayatilaka [10]	Human cadavers (10)	LM	
1968	Hayreh [6]	Monkeys and rabbits	Macroscopy	Fundoscopy, CSF pressure
1993	Liu [16]	Human cadavers (6)	Macroscopy	Subarachnoid pressure measurement
1999	Killer [11]	Human cadavers (7)	LM and EM	
2001	Huna-Baron [8]	Patients (15)		Visual acuity, visual field, lumbar puncture and pressure, MRI
2003	Killer [12]	Human cadavers (9)	EM	
2006	Killer [13]	Patients (6)		Lumbar puncture and pressure/Fundoscopy/MRI
2007	Killer [14]	Patients (5)		CT-cisternography with Valsalva manoeuvre, CSF analysis
2010	Jaggi [9]	Sheeps (7)	LM and EM	
2018	Pircher [19]	Patients (16)		CT-cisternography
2021	Tsutsumi [21]	Patients (89), human cadavers (10)	Macroscopy	MRI

The present study has limitations. The main, is that it is carried out in a postmortem condition which does not reflect the physiological conditions of CSF flow within the SAS. In addition, subarachnoid staining by MB injection was performed by a single observer without objective measurement of intracranial pressure at the time of injection. This may have been done with too little pressure, making the flow to the ONS less efficient, or too high, forcing the flow of the CSF.

The postmortem study also impacted the quality of the tissues analyzed. However, the collagen fibers were well-preserved despite postmortem analyzes and numerous laboratory manipulations.

Our analysis, in EM, was performed only approximately at 4 mm from the posterior pole of the eyeball and we did not compare these results to other locations of the ONS. It might be interesting to compare the structure of the SAS with that of the end of SAS near to the papilla and further back, near to the optic canal, to search for parts more compartmentalized than others.

Macroscopically, in SAS of the ONS, we found inter-individual and intra-individual variability (bilateral and/or within the same ONS), however, the analysis was carried out on a small number of specimens and the density measurement of the arachnoid trabecular meshwork was subjective, carried out by a single observer. To perform a more reliable analysis, it would have been interesting to use a density scale by measuring the average mesh size on a given surface and to make a cross-assessment with another observer.

In clinical practice, we have limited explanations of asymmetric papilledema or its absence in certain ICH. Indeed, all the arachnoid structures described in our study are so delicate that they cannot be visualized by CT, MRI, or ultrasound. We suppose that there are micro-partitions in the SAS of the ONS which sometimes alter the ophthalmological presentation of the ICH. Papilledema in IIH is one of the cardinal signs looked for [4]. However, in view of the literature and our results, an asymmetric papilledema or its absence should not formally rule out the diagnosis of IIH.

Conclusion

Our anatomical study investigated the SAS of the ONS by a macroscopic, light and electron microscopic study. We described the structure, the staining, and the variability of the SAS around the ON in its intraorbital segment. Macroscopic analysis showed inter-individual and intra-individual variability and the staining showed a partial progression of MB in the SAS. Macroscopic and microscopic results revealed a composition rich in arachnoid trabeculae and septa which seem to form some partitions. EM analysis confirmed the dense collagen composition of the arachnoid trabeculae, organized in thick fibers. This study could contribute to improve the understanding of the pathophysiologic mechanism of asymmetric or unilateral or absent papilledema in certain ICH.

Author contributions Conception and design: AD, DL. Dissection and acquisition of data: AD. Analysis and interpretation of data: AD, VJ, DL. Drafting the article: AD. Critically revising the article: VJ, DL, MS, LLP. Reviewed submitted version of manuscript: AD.

Declarations

Conflict of interest The authors declare no conflict of interest. Bordeaux Imaging Center has received research grants from Laboratory Anatomy of Bordeaux to finance EM analyzes.

Ethical approval All procedures performed in study were in accordance with the 1964 Helsinki Declaration and its later amendments or comparable ethical standards.

References

1. Banerjee M, Aalok SP, Vibha D (2020) Unilateral papilledema in idiopathic intracranial hypertension: a rare entity. Eur J Ophthalmol. https://doi.org/10.1177/1120672120969041
2. Bidot S, Bruce BB, Saindane AM, Newman NJ, Biousse V (2015) Asymmetric papilledema in idiopathic intracranial hypertension. J Neuroophthalmol 35:31–36. https://doi.org/10.1097/WNO.0000000000000205
3. Francois P, Lescanne E, Velut S (2011) The dural sheath of the optic nerve: descriptive anatomy and surgical applications. In: Pickard JD, Akalan N, Benes V, Di Rocco C, Dolenc VV, Antunes JL, Schramm J, Sindou M (eds) Advances and technical standards in neurosurgery. Springer Vienna, Vienna, pp 187–198
4. Friedman DI, Liu GT, Digre KB (2013) Revised diagnostic criteria for the pseudotumor cerebri syndrome in adults and children. Neurology 81:1159–1165. https://doi.org/10.1212/WNL.0b013e3182a55f17
5. Geeraerts T, Newcombe VF, Coles JP, Abate M, Perkes IE, Hutchinson PJ, Outtrim JG, Chatfield DA, Menon DK (2008) Use of T2-weighted magnetic resonance imaging of the optic nerve sheath to detect raised intracranial pressure. Crit Care 12:R114. https://doi.org/10.1186/cc7006
6. Hayreh SS (1968) Pathogenesis of oedema of the optic disc. Doc Ophthalmol 24:289–411. https://doi.org/10.1007/BF02550944
7. Hayreh SS (2016) Pathogenesis of optic disc edema in raised intracranial pressure. Prog Retin Eye Res 50:108–144. https://doi.org/10.1016/j.preteyeres.2015.10.001
8. Huna-Baron R, Landau K, Rosenberg M, Warren FA, Kupersmith MJ (2001) Unilateral swollen disc due to increased intracranial pressure. Neurology 56:1588–1590. https://doi.org/10.1212/WNL.56.11.1588
9. Jaggi GP, Harlev M, Ziegler U, Dotan S, Miller NR, Killer HE (2010) Cerebrospinal fluid segregation optic neuropathy: an experimental model and a hypothesis. Br J Ophthalmol 94:1088–1093. https://doi.org/10.1136/bjo.2009.171660
10. Jayatilaka ADP. A note on arachnoid villi in relation to human optic nerves. 3
11. Killer HE (1999) Lymphatic capillaries in the meninges of the human optic nerve. J Neuro-ophtalmol 19(4):222–228

12. Killer HE (2003) Architecture of arachnoid trabeculae, pillars, and septa in the subarachnoid space of the human optic nerve: anatomy and clinical considerations. Br J Ophthalmol 87:777–781. https://doi.org/10.1136/bjo.87.6.777
13. Killer HE, Jaggi GP, Flammer J, Miller NR, Huber AR (2006) The optic nerve: a new window into cerebrospinal fluid composition? Brain 129:1027–1030. https://doi.org/10.1093/brain/awl045
14. Killer HE, Jaggi GP, Flammer J, Miller NR, Huber AR, Mironov A (2007) Cerebrospinal fluid dynamics between the intracranial and the subarachnoid space of the optic nerve. Is it always bidirectional? Brain 130:514–520. https://doi.org/10.1093/brain/awl324
15. Klinge PM, McElroy A, Donahue JE, Brinker T, Gokaslan ZL, Beland MD (2021) Abnormal spinal cord motion at the craniocervical junction in hypermobile Ehlers–Danlos patients. J Neurosurg Spine 35:18–24. https://doi.org/10.3171/2020.10.SPINE201765
16. Liu D, Kahn M (1993) Measurement and relationship of subarachnoid pressure of the optic nerve to intracranial pressures in fresh cadavers. Am J Ophthalmol 116:548–556. https://doi.org/10.1016/S0002-9394(14)73195-2
17. Mienaltowski MJ, Birk DE (2014) Structure, physiology, and biochemistry of collagens. In: Halper J (ed) Progress in heritable soft connective tissue diseases. Springer Netherlands, Dordrecht, pp 5–29
18. Passi N, Degnan AJ, Levy LM (2013) MR imaging of papilledema and visual pathways: effects of increased intracranial pressure and pathophysiologic mechanisms. AJNR Am J Neuroradiol 34:919–924. https://doi.org/10.3174/ajnr.A3022
19. Pircher A, Montali M, Pircher J, Berberat J, Remonda L, Killer HE (2018) Perioptic cerebrospinal fluid dynamics in idiopathic intracranial hypertension. Front Neurol. https://doi.org/10.3389/fneur.2018.00506
20. Selhorst J, Chen Y (2009) The optic nerve. Semin Neurol 29:029–035. https://doi.org/10.1055/s-0028-1124020
21. Tsutsumi S, Ono H, Ishii H (2021) Hyperintense areas in the intraorbital optic nerve evaluated by T2-weighted magnetic resonance imaging: a glymphatic pathway? Surg Radiol Anat 43:1273–1278. https://doi.org/10.1007/s00276-020-02649-7
22. Watanabe A, Kinouchi H, Horikoshi T, Uchida M, Ishigame K (2008) Effect of intracranial pressure on the diameter of the optic nerve sheath. JNS 109:255–258. https://doi.org/10.3171/JNS/2008/109/8/0255